


Iron-sulfur cluster carrier proteins involved in the assembly of *Escherichia coli* NADH:ubiquinone oxidoreductase (complex I)

Sabrina Burschel,¹ Doris Kreuzer Decovic,^{1,2}
Franziska Nuber,¹ Marie Stiller,¹ Maud Hofmann,¹
Arkadiusz Zupok,³ Beata Siemiatkowska,⁴
Michal Gorka,⁴ Silke Leimkühler³ and
Thorsten Friedrich ^{1,2*}

¹Albert-Ludwigs-Universität, Institut für Biochemie,
Albertstr. 21, D-79104, Freiburg, Germany.

²Spemann Graduate School of Biology and Medicine
(SGBM), University of Freiburg, Germany.

³University of Potsdam, Institut für Biochemie und
Biologie, Karl-Liebknecht-Str. 24-25, 14476, Potsdam-
Golm, Germany.

⁴Max-Planck-Institute of Molecular Plant Physiology, Am
Mühlenberg 1, 14476, Potsdam-Golm, Germany.

Summary

The NADH:ubiquinone oxidoreductase (respiratory complex I) is the main entry point for electrons into the *Escherichia coli* aerobic respiratory chain. With its sophisticated setup of 13 different subunits and cofactors it is anticipated that various chaperones are needed for its proper maturation. However, very little is known about the assembly of *E. coli* complex I, especially concerning the incorporation of the iron-sulfur clusters. To identify iron-sulfur cluster carrier proteins possibly involved in the process, we generated knockout strains of NfuA, BoIA, YajL, Mrp, GrxD and IbaG that have been reported either to be involved in the maturation of mitochondrial complex I or to exert influence on the clusters of bacterial complex. We determined the NADH and succinate oxidase activities of membranes from the mutant strains to monitor the specificity of the individual mutations for complex I. The deletion of NfuA, BoIA and Mrp led to a decreased stability and partially disturbed assembly of the complex as determined by sucrose gradient centrifugation and native PAGE. EPR spectroscopy of cytoplasmic

membranes revealed that the BoIA deletion results in the loss of the binuclear Fe/S cluster N1b.

Introduction

Iron-sulfur (Fe/S) clusters are among the most important, versatile and ancient cofactors in nature. They are present in all kingdoms of life participating in electron transfer reactions, respiration, photosynthesis, DNA repair, gene regulation and other processes (Kiley and Beinert, 2003; Roche *et al.*, 2013; Braymer and Lill, 2017). The clusters are fabricated by evolutionary conserved biosynthetic machineries (Roche *et al.*, 2013; Py and Barras, 2015) called NIF (from nitrogen fixation), SUF (from sulfur mobilization) and ISC (from iron-sulfur cluster) (Takahashi and Tokumoto, 2002; Ayala-Castro *et al.*, 2008; Py and Barras, 2010). While the NIF system is exclusively required for nitrogenase maturation, ISC and SUF are generally used for the biogenesis of Fe/S proteins. ISC is the dominant housekeeping system that is inactivated by reactive oxygen species. SUF is expressed when bacteria grow under oxidative stress or iron limitation. Both systems share a common mechanism comprising three major steps (Supporting Information, Fig. S1). A cysteine desulfurase (IscS and SufS) removes sulfur from L-cysteine and delivers it to the scaffold protein IscU (Zheng and Dean, 1994; Schwartz *et al.*, 2000; Mihara and Esaki, 2002). On IscU, sulfur and iron that provided by a still unknown source are assembled into a cluster. The cluster is released from the scaffold protein by an ATP-hydrolyzing component and is further transferred to the individual apo-proteins either directly or by means of A-type carriers (ATCs) (Nachin *et al.*, 2003; Vinella *et al.*, 2009). *Escherichia coli* encodes three ATCs namely ErpA, IscA and SufA that are classified as Fe/S cluster carrier proteins because they do not interact with cysteine desulfurases (Angelini *et al.*, 2008; Tan *et al.*, 2009). The putative Fe/S cluster carrier NfuA contains an amino-terminal domain similar to an ATC but lacks the cysteine residues involved in cluster binding. It is discussed that this degenerated ATC domain enables NfuA to be targeted to its apoproteins (Agar *et al.*, 2000; Dos Santos *et al.*, 2004; Smith *et al.*, 2005; Bandyopadhyay

Accepted 19 September, 2018. *For correspondence. E-mail friedrich@bio.chemie.uni-freiburg.de; Tel. +49 (0)761 203 6060; Fax +49 (0)761 203 6096.

et al., 2008; Jin *et al.*, 2008). Recently, it was shown that NfuA reconstitutes the Fe/S cluster of lipoyl synthase to restore its catalytic activity (McCarthy and Booker, 2017).

Other *E. coli* proteins share sequence homology to eukaryotic proteins that were identified to participate in Fe/S cluster delivery. One of these is Mrp of the ParA-like family (Koonin, 1993; Hausmann *et al.*, 2005; Boyd *et al.*, 2008) and the monothiol glutaredoxin GrxD. It is proposed that homodimeric GrxD binds binuclear Fe/S clusters, but that it also acts as a heterodimer with BolA, a poorly characterized protein involved in shaping cell morphology and regulatory processes under stress conditions (Yeung *et al.*, 2011; Li and Outten, 2012). Both, the GrxD homodimer and the GrxD/BolA heterodimer are capable of delivering Fe/S cluster to an acceptor protein. Together with Nfu, Bol is involved in the biogenesis of mitochondrial Fe/S clusters (Melber *et al.*, 2016; Uzarska *et al.*, 2016). It was suggested that another *E. coli* BolA-like protein, IbaG, might also be involved in Fe/S cluster trafficking (Dlouhy *et al.*, 2016). Although the participation of these proteins in Fe/S cluster delivery is shown, their target proteins remain largely unknown.

One of the major target proteins is the energy-converting NADH:ubiquinone oxidoreductase, respiratory complex I. Complex I is the first enzyme of respiratory chains in many eukaryotes and most bacteria (Baradaran *et al.*, 2013; Zickermann *et al.*, 2015; Fiedorczuk *et al.*, 2016; Zhu *et al.*, 2016). Homologues of the complex are present in all domains of life and contribute to the generation of the proton motive force essential to drive energy-consuming processes (Friedrich, 2014). A dysfunction or incomplete assembly of the human complex is associated with the onset of neurodegenerative diseases such as Parkinson's syndrome (Lin and Beal 2006; Rhein *et al.*, 2009; Baertling *et al.*, 2017). In patients with Friedreich's ataxia, non-functional Fe/S proteins and local iron accumulation have been observed that are caused by a mutation of the gene encoding frataxin (Bidichandani and Delatycki, 1998; Isaya, 2014). Frataxin is discussed to be the source of iron for the scaffold protein, although it was shown that it is not essential for the biogenesis of *E. coli* complex I (Pohl *et al.*, 2007a).

The closest *E. coli* homolog of the Parkinsonism-associated protein DJ-1, YajL, was proposed to play a role in the prevention of protein aggregation. YajL is a multi-functional oxidative stress response protein that exhibits chaperone activity (Sasstry *et al.*, 2002; Gautier *et al.*, 2012). It was reported that deletion of *yajL* leads to a decrease complex I activity and an overproduction of alternative dehydrogenases (Messouadi *et al.*, 2015).

E. coli complex I is made up of 13 different subunits called NuoA-N (Friedrich *et al.*, 2016). They are assembled to a peripheral arm protruding into the cytoplasm and a membrane arm embedded in the cytoplasmic membrane

(Baradaran *et al.*, 2013). The peripheral arm catalyzes NADH oxidation, electron transfer to the quinone and participates in quinone reduction. Electron transfer is accomplished by one flavin mononucleotide (FMN) and nine Fe/S clusters (de Vries *et al.*, 2015). NADH is oxidized by FMN and the electrons are transferred to the substrate quinone by a 95 Å long chain of seven Fe/S clusters. The chain comprises the tetranuclear cluster N3 on NuoF and the binuclear N1b on NuoG. NuoG contains two additional tetranuclear clusters that have not yet been unequivocally assigned to distinct EPR signals (Yakovlev *et al.*, 2007; Ohnishi and Nakamaru-Ogiso, 2008). The third tetranuclear Fe/S cluster on NuoG, N7, is only found in a few bacterial species and is not involved in electron transfer (Pohl *et al.*, 2007b). Electrons are further transferred from NuoG to quinone *via* three tetranuclear Fe/S clusters located on NuoI and NuoB. An additional binuclear cluster on NuoE, N1a, is not part of the chain of clusters but is located in electron transfer distance to FMN. The cluster is strictly conserved and plays not only a role in the stability and the assembly of the complex (Birrell *et al.*, 2013; Dörner *et al.*, 2017) but also in regulating NADH oxidation (Gnandt *et al.*, 2017).

Here, we analyzed whether NfuA, Mrp, YajL, IbaG, GrxD and BolA are involved in the incorporation of Fe/S clusters in *E. coli* complex I by generating knockout strains that were examined for their specific complex I activity. It turned out that Mrp has a significant effect on complex I activity and assembly, while the deletion of NfuA did not only affect the activity of complex I, but also that of respiratory complex II containing three Fe/S clusters. In addition, BolA seems to be important for the incorporation of N1b into complex I.

Results

Generation of deletion strains and cell growth

E. coli encodes two membrane bound NADH dehydrogenases, namely, respiratory complex I (encoded by the *nuo*-genes) and the alternative NADH dehydrogenase (encoded by the *ndh*-gene) (Uندن *et al.*, 2014). To directly measure complex I activity in the membranes and to circumvent the use of highly expensive deamino (d)-NADH as substrate, BW25113 Δndh was used as parental strain. D-NADH is an artificial substrate with a pronounced selectivity for complex I over the alternative NADH dehydrogenase (Friedrich *et al.*, 1994). To analyze whether the loss of the alternative NADH dehydrogenase might compromise the growth of mutant strains lacking the putative Fe/S cluster carrier proteins, strains BW25113 Δndh , BW25113 Δnuo and BW25113 $\Delta ndh \Delta nuo$ were generated and their growth on minimal medium using acetate as non-fermentable carbon

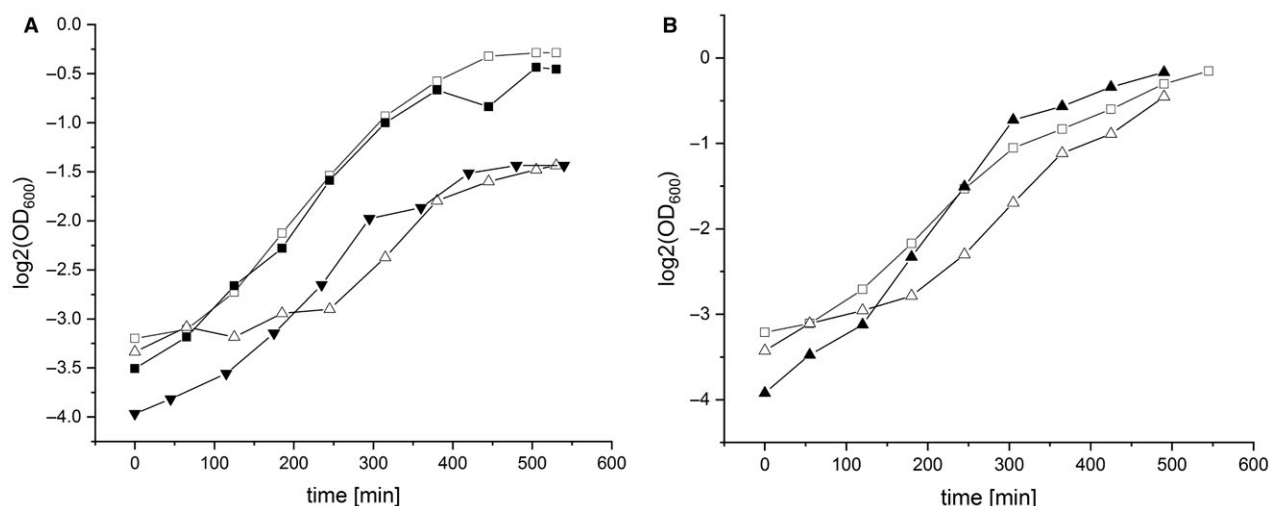


Fig. 1. Growth of the NADH dehydrogenase deletion strains on minimal media with acetate as sole carbon source.

A. Growth of BW25113 (full squares), BW25113 Δndh (open squares), BW25113 Δnuo (full triangles) and the double deletion strain BW25113 $\Delta ndh \Delta nuo$ (open triangles).

B. Growth of BW25113 Δndh (open squares), BW25113 $\Delta ndh \Delta grxD/pET$ (open triangles) and BW25113 $\Delta ndh \Delta grxD/pET grxD$ (full triangles). The *mrp*, *nfuA* and *bolA* deletion strains grew like BW25113 $\Delta ndh \Delta grxD/pET$. Growth of these strains was restored by the transformation with the lacking gene on the plasmid.

Table 1. NADH and d-NADH oxidase activity of cytoplasmic membranes of *E. coli* BW25113 lacking complex I (Δnuo), the alternative NADH dehydrogenase (Δndh) or both ($\Delta ndh \Delta nuo$).

Membranes isolated from strains	NADH oxidase activity [U mg ⁻¹]	%	d-NADH oxidase activity [U mg ⁻¹]	%
BW25113	0.36 ± 0.03	100	0.18 ± 0.02	100
BW25113 Δndh	0.18 ± 0.02	50	0.17 ± 0.02	95
BW25113 Δnuo	0.07 ± 0.01	38	0	0
BW25113 $\Delta ndh \Delta nuo$	0	0	0	0

source was compared with that of the parental strain, BW25113 (Fig. 1A). Strain BW25113 Δndh grew virtually identical to the parental strain, while the deletion of the *nuo* genes led to significantly decreased growth rate. Deletion of both, the *ndh*- and the *nuo*-genes, had the same effect as deleting *nuo* (Fig. 1A). The strains lacking the *nuo*-genes grew slower most likely due to an imbalanced NADH/NAD⁺ ratio hampering the TCA cycle. It is known that the alternative NADH dehydrogenase has an approximately 10-fold lower affinity to NADH than complex I (Friedrich *et al.*, 1994). The deletions had no effect on the growth of the strains with glucose as sole carbon source (Supporting Information, Fig. S2). Thus, a disturbed function of complex I is detectable in strain BW25113 independent of the presence of Δndh .

The NADH oxidase activity of the parental strain involves the activity of both membrane-bound NADH dehydrogenases (Table 1), while the d-NADH oxidase activity is solely mediated by complex I (Friedrich *et al.*, 1994). The d-NADH oxidase activity of membranes from strain BW25113 was 50% of the NADH oxidase activity.

The NADH oxidase activity was inhibited by 45% by an addition of 10 μ M piericidin A, a specific complex I inhibitor. Thus, both enzymes contribute approximately an equal share to the NADH oxidase activity. The d-NADH oxidase activity was completely lost in strains lacking the *nuo*-genes indicating the specificity of the substrate (Table 1). The *ndh* deletion did not significantly affect the d-NADH oxidase activity. Furthermore, no NADH and d-NADH oxidase activity was detectable in a strain lacking both NADH dehydrogenases indicating that no other protein contributes to this activity (Table 1). Thus, NADH is exclusively used by complex I in strain BW25113 Δndh turning it into an excellent host strain to generate chromosomal deletions of genes encoding putative Fe/S cluster carrier proteins. Double or triple deletion strains were individually transformed with pETblue-1 (*mrp/nfuA/yajL/bolA/ibaG/grxD*) to complement the corresponding deletions. Noteworthy, we were unable to delete *erpA* from the chromosome despite numerous attempts confirming that it is essential for the viability of *E. coli* under aerobic growth conditions (Loiseau *et al.*, 2007).

Table 2. NADH and succinate oxidase activity of cytoplasmic membranes of various *E. coli* mutant strains. The activities are given in percentage of the activity of the parental strain.

Membranes isolated from strains	NADH oxidase activity [U mg ⁻¹]	%	Succinate oxidase activity [U mg ⁻¹]	%
BW25113 Δndh	0.18 ± 0.02	100	0.045 ± 0.005	100
BW25113 $\Delta ndh \Delta bolA$	0.16 ± 0.02	90	0.050 ± 0.005	111
BW25113 $\Delta ndh \Delta bolA/pETblue-1 bolA$	0.18 ± 0.02	100	0.056 ± 0.006	124
BW25113 $\Delta ndh \Delta yajL$	0.14 ± 0.01	78	0.035 ± 0.004	78
BW25113 $\Delta ndh \Delta yajL/pETblue-1 yajL$	0.26 ± 0.03	144	0.059 ± 0.006	131
BW25113 $\Delta ndh \Delta nfuA$	0.09 ± 0.01	50	0.030 ± 0.003	67
BW25113 $\Delta ndh \Delta nfuA/pETblue-1 nfuA$	0.16 ± 0.02	89	0.038 ± 0.004	84
BW25113 $\Delta ndh \Delta mrp$	0.10 ± 0.01	56	0.043 ± 0.004	96
BW25113 $\Delta ndh \Delta mrp/pETblue-1 mrp$	0.20 ± 0.02	111	0.075 ± 0.008	167
BW25113 $\Delta ndh \Delta grxD$	0.17 ± 0.02	97	0.034 ± 0.004	75
BW25113 $\Delta ndh \Delta grxD/pETblue-1 grxD$	0.13 ± 0.01	70	0.056 ± 0.006	125
BW25113 $\Delta ndh \Delta ibaG$	0.18 ± 0.02	100	0.042 ± 0.004	93
BW25113 $\Delta ndh \Delta grxD \Delta ibaG$	0.19 ± 0.02	105	0.039 ± 0.004	88
BW25113 $\Delta ndh \Delta bolA \Delta ibaG$	0.15 ± 0.01	86	0.021 ± 0.002	47
BW25113 $\Delta ndh \Delta bolA \Delta ibaG/pETblue-1 bolA$	0.20 ± 0.02	111	0.050 ± 0.005	112
BW25113 $\Delta ndh \Delta bolA \Delta ibaG/pETblue-1 ibaG$	0.21 ± 0.02	114	0.036 ± 0.004	79
BW25113 $\Delta ndh \Delta bolA \Delta grxD$	0.15 ± 0.01	86	0.027 ± 0.003	59
BW25113 $\Delta ndh \Delta bolA \Delta grxD/pETblue-1 bolA$	0.14 ± 0.01	78	0.041 ± 0.004	90
BW25113 $\Delta ndh \Delta bolA \Delta grxD/pETblue-1 grxD$	0.09 ± 0.01	48	0.034 ± 0.003	79
BW25113 $\Delta ndh \Delta bolA \Delta grxD \Delta ibaG$	0.12 ± 0.01	65	0.021 ± 0.002	47

The double deletion strains were grown in minimal medium with acetate as carbon source (Fig. 1B). BW25113 $\Delta ndh \Delta yajL$ and BW25113 $\Delta ndh \Delta ibaG$ grew like the parental strain (data not shown), while the other deletion strains showed a decreased growth rate. Complementation of these strains with a *bolA*, *mrp*, *nfuA*, *grxD* plasmid restored growth (Fig. 1B).

Activity of complex I and II in the mutant strains

Cells were disrupted by two passes through a French pressure cell and cytoplasmic membranes were obtained by differential centrifugation (Leif *et al.*, 1995). The activity of the aerobic respiratory chain was measured with a Clark-type electrode as decrease in oxygen concentration (John, 1976). The reaction was either started by an addition of NADH or succinate. The NADH oxidase activity reflects the activity of complex I due to the chromosomal deletion of *ndh* coding the alternative NADH dehydrogenase. The succinate oxidase activity is mediated by succinate:ubiquinone oxidoreductase, respiratory complex II, containing three Fe/S clusters (Yankovskaya *et al.*, 2003). This activity was used as control to determine the specificity of the deletions with respect to complex I. Parental strain BW25113 Δndh was used as reference and the activities obtained with the mutant's membranes were expressed as percentage of the activity of the parental strain (Table 2).

Strain BW25113 $\Delta ndh \Delta bolA$ showed no significant change of NADH and succinate oxidase activities, while both were slightly but significantly decreased by 20%

in strain BW25113 $\Delta ndh \Delta yajL$. Deletion of *yajL* was reported to result in an upregulation of other dehydrogenases (Messouadi *et al.*, 2015). Indeed, the formate oxidase activity caused by the formate dehydrogenase expressed under oxic conditions (Fdh-O) was with 0.18 U mg⁻¹ in the $\Delta yajL$ deletion strain twice the value obtained with the parental strain.

NADH oxidase activity of membranes from BW25113 $\Delta ndh \Delta nfuA$ and $\Delta ndh \Delta mrp$ was approximately halved. While the loss of NfuA also decreased the succinate oxidase activity by one-third, the lack of Mrp had no influence on the latter activity suggesting that Mrp is specifically needed for the incorporation of Fe/S clusters into complex I. The lack of GrxD did not significantly influence NADH oxidase activity, however, resulted in a succinate oxidase activity that was diminished by one quarter. The deletion of *ibaG* had neither an effect on the NADH nor on the succinate oxidase activity (Table 2).

Deletion strains with decreased oxidase activity were individually transformed with plasmids containing the chromosomally deleted *yajL*, *mrp* and *nfuA* respectively, (Table 2). The pET vector was chosen due to its leaky gene expression in the absence of any inducer in a medium lacking glucose (Hattab *et al.*, 2015). Noteworthy, the knockout strains complemented with *yajL* and *mrp* showed a significantly enhanced NADH and succinate oxidase activity (Table 2) suggesting that the amount of a functional complex I and II may be limited by the incorporation of Fe/S clusters into the enzyme complexes in *E. coli*. *In trans* complementation with *nfuA* also significantly increased both activities in the deletion strain.

It was shown that BolA and IbaG, both members of the BolA-protein family, are capable of forming heterodimers with GrxD bridging a [2Fe-2S] cluster (Yeung *et al.*, 2011; Dlouhy *et al.*, 2016). To monitor whether the proteins of the BolA family and GrxD may substitute each other, triple deletion strains lacking *ndh* were constructed (Table 2). The strain devoid of *grxD* and *ibaG* showed no significant change in NADH oxidase activity. Strains lacking *bolA/grxD* and *bolA/ibaG* exhibited a slightly decreased NADH oxidase activity that was most likely solely due to the lack of BolA leading to a similarly diminished activity (Table 2). The triple deletion strains showed no additive effects on NADH oxidase activities opposing a possible substitution of BolA by IbaG and by GrxD. However, the NADH oxidase activity of a strain carrying the quadruple deletion *ndh*, *bolA*, *grxD* and *ibaG* was significantly reduced by one third suggesting that IbaG and GrxD together might be capable of compensating the loss of BolA.

The succinate oxidase activity of the strain lacking *grxD/ibaG* was reduced to the same amount as found with the individual deletions (Table 2). However, the succinate oxidase activity of strains lacking *bolA/grxD* and *bolA/ibaG* was significantly decreased compared to that of the strains individually lacking *bolA*, *grxD* or *ibaG* (Table 2). Correspondingly, interplay of these proteins seems to be important for the incorporation of Fe/S clusters in complex II. The quadruple deletion of *ndh*, *bolA*, *grxD* and *ibaG* diminished the succinate oxidase activity to the same extent as the *ndh*, *bolA* and *ibaG* deletion (Table 2).

Triple deletion strains with diminished NADH oxidase activity were individually complemented with the corresponding pET vectors. BW25113 $\Delta ndh \Delta bolA \Delta ibaG$ complemented either with *ibaG* or *bolA* showed a slightly

higher NADH oxidase activity than the parental strain. Complementation of the strain with *bolA* led to the full recovery of succinate oxidase activity. However, complementation with *ibaG* alone was not sufficient to recover activity (Table 2). BW25113 $\Delta ndh \Delta bolA \Delta grxD$ complemented with *bolA* exhibited a slightly lower NADH and a clearly increased succinate oxidase activity. Complementation of this strain with *grxD* led to a slight enhancement of succinate oxidase activity. Most surprisingly, this strain repeatedly exhibited further decreased NADH oxidase activity (Table 2). The same observation was made by using a strain from the Keio collection, in which *grxD* gene is inactivated (*grxD::nptI*) and complemented with a pCA24N_{his}*grxD* from the ASKA collection (<https://cgsc2.biology.yale.edu/KeioList.php>).

Assembly of complex I in the mutant strains

Assembly of complex I in the various mutant strains was investigated by extracting proteins from cytoplasmic membranes with dodecyl-maltoside and loading the cleared extract on a native PAGE (Fig. 2) and a sucrose gradient (Fig. 3).

Isolated *E. coli* complex I and the soluble NADH dehydrogenase fragment of the complex consisting of subunits NuoE, F and G (Braun *et al.*, 1998) were used as standards to determine the position of the fully assembled complex I and the defined fragment (Fig. 2). As control, a membrane extract from the strain lacking both NADH dehydrogenases was also applied. Assemblies of the complex that contain NuoF were identified by in-gel staining with nitroblue tetrazolium (NBT) and NADH. The NADH dehydrogenase activity leads to the precipitation of blue formazan in the gel (Zerbetto *et al.*, 1997). Due

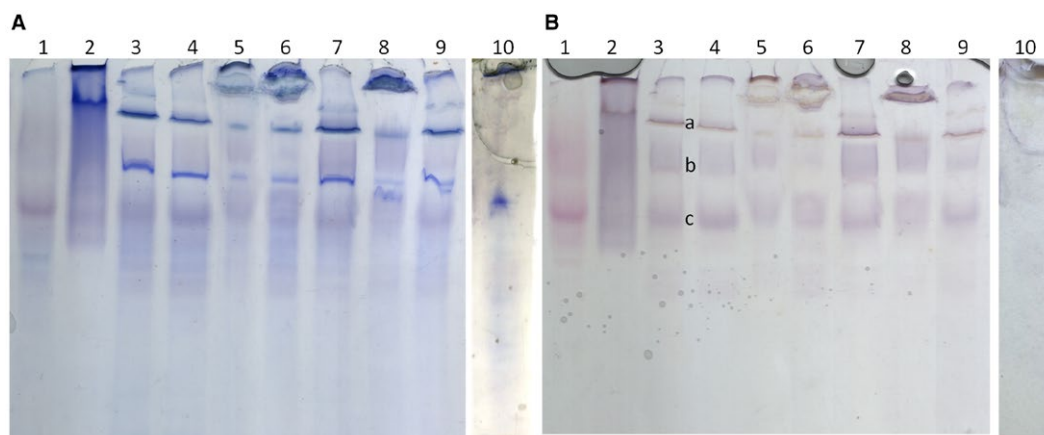


Fig. 2. Coomassie blue A. and NADH/NBT B. stained native PA gradient gel loaded with membrane extracts from *E. coli* deletion strains. 40 μ g of the membrane extract from BW25113 Δndh (3), BW25113 $\Delta ndh \Delta bolA$ (4), BW25113 $\Delta ndh \Delta mrp$ (5), BW25113 $\Delta ndh \Delta nfua$ (6), BW25113 $\Delta ndh \Delta yajL$ (7), BW25113 $\Delta ndh \Delta grxD$ (8), BW25113 $\Delta ndh \Delta ibaG$ (9) and BW25113 $\Delta ndh \Delta nuo$ (10) were loaded on a 3.5–16% acrylamide gel in a pH 6.3 buffer. Isolated NADH dehydrogenase fragment consisting of NuoE, F and G (1) and isolated *E. coli* complex I (2) were applied as references. The bands discussed in the text are a) complex I, b) novel, 300 kDa fragment and c) NADH dehydrogenase fragment as indicated in lane B3.

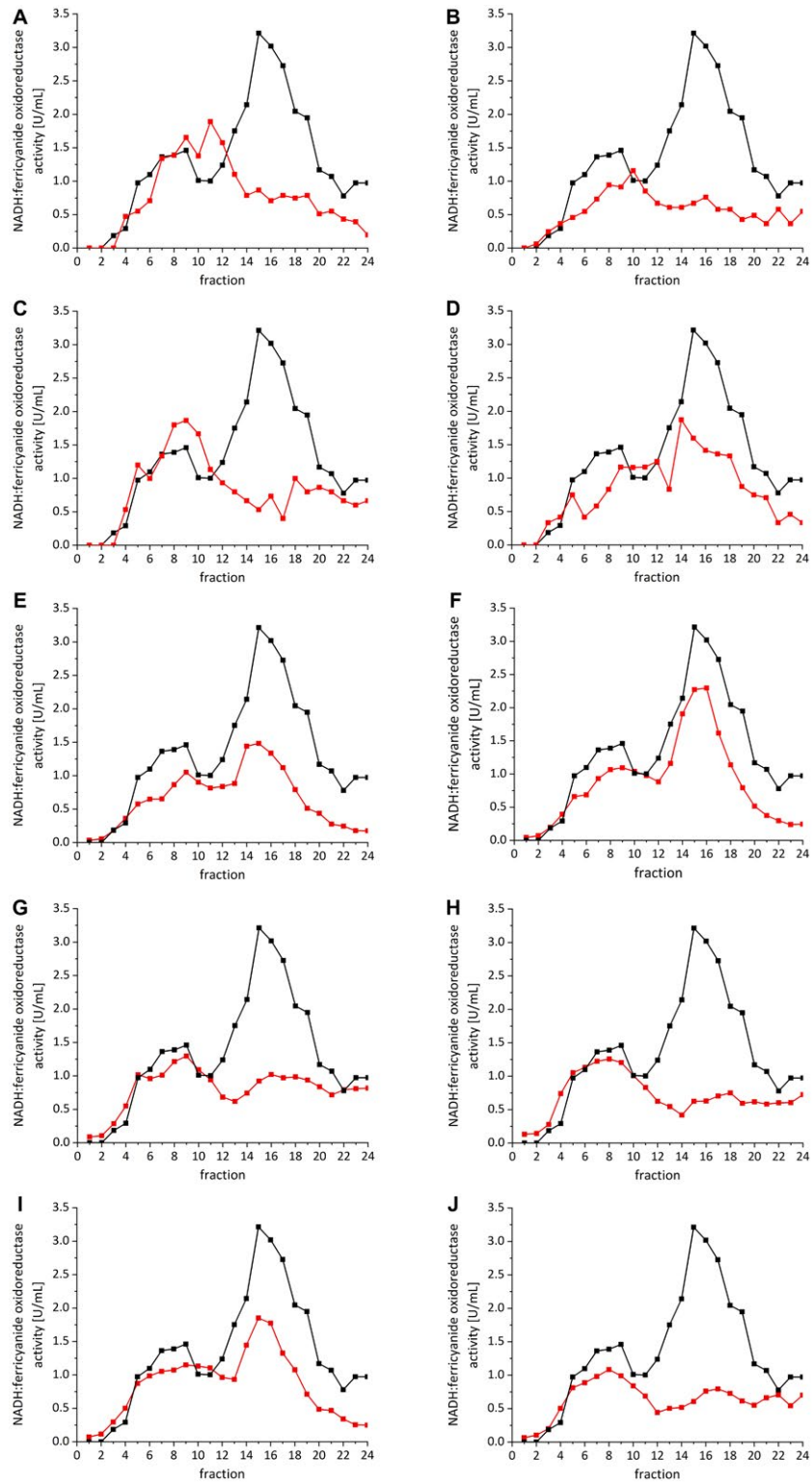


Fig. 3. Sucrose gradient of detergent-solubilized membranes from various *E. coli* strains. The NADH/ferricyanide oxidoreductase activity of fractions from gradients loaded with detergent extracts from BW25113 Δndh (black), from the double knockout strains A. $\Delta nfuA$, B. Δmmp , C. $\Delta boIA$, D. $\Delta yajL$, E. $\Delta grxD$, F. $\Delta ibaG$, from the triple knockout strains G. $\Delta boIA \Delta grxD$, H. $\Delta boIA \Delta ibaG$ and I. $\Delta ibaG \Delta grxD$ and the quadruple knockout strain J. $\Delta boIA \Delta ibaG \Delta grxD$ (all in red). The activities were normalized to 20 mg membrane protein extract applied per gradient.

to the lack of the alternative NADH dehydrogenase in the parental strain there is no other enzyme in the *E. coli* cytoplasmic membrane comprising this activity (Table 1).

The fully assembled complex with an apparent molecular mass of 550 kDa was clearly detectable in the membrane extract from the parental strain and from strains lacking *bolA*, *yajL* and *ibaG* (Fig. 2). The amount of proteins was significantly diminished in the membranes of the strains lacking *mrp*, *nfuA* and *grxD* (Fig. 2). Proteins were hardly detectable neither by Coomassie nor by NBT staining. It seemed that proteins from these strains tend to precipitate in the sample wells. Nevertheless GrxD, Mrp and NfuA are important to guarantee the assembly of a stable *E. coli* complex I as the band of fully assembled complex I was hardly detectable by NBT-staining in the lanes loaded with the extract of the corresponding mutants. The NADH dehydrogenase fragment with an apparent molecular mass of about 170 kDa was detectable in all samples by NBT staining indicating a partial degradation of the complex under the experimental condition.

Unexpectedly, an additional broad band was present in the extracts from all strains after NBT-staining of the gel (Fig. 2). This fragment has so far not been described and its subunit composition is not known. With its apparent molecular mass of about 300 kDa it might represent the entire peripheral arm of the complex probably attached to some of the hydrophobic subunits. To identify its subunit composition, the band was sliced out from the native gel and subjected to SDS-PAGE. The SDS gel was cut in discrete stripes that were further analyzed by mass spectrometry (Supporting Information, Fig. S3). All subunits of complex I were identified in the SDS gel with the exception of NuoL and NuoM of the membrane arm. In addition, NuoN was only detectable in faint amounts (Supporting Information, Fig. S3). It appears that this band reflects a fragment of the complex lacking the distal part of the membrane arm made up by subunits NuoL, M and N (Baradaran *et al.*, 2013). A similar fragment was described by electron microscopy of *E. coli* complex I (Baranova *et al.*, 2007). This incomplete complex was detectable in the parental strain suggesting that it does not derive from the deletion of the putative cluster carrier proteins and it remains unclear whether it represents an assembly intermediate of the complex or a product of the decay of the complex due to detergent extraction. Furthermore, mass spectrometry revealed the presence of NfuA in the same band as NuoG after SDS-PAGE (Supporting Information, Fig. S3). NfuA was also detected in slices covering the expected molecular mass of the protein around 21 kDa.

A cleared extract obtained from incubating the membranes for 1 h with 1% detergent was loaded onto 24 ml sucrose gradients and the membrane proteins contained were separated by ultracentrifugation. The gradients were

fractionated in 1 ml portions and their NADH/ferricyanide oxidoreductase activity was measured (Fig. 3). The activity is solely caused by the FMN containing subunit NuoF. The fully assembled complex I sediments in fractions 13–18 under chosen conditions (Leif *et al.*, 1995) as seen in the activity profile of the gradient loaded with the extract of the parental strain (Fig. 3). In addition, a broad activity peak was detected around fraction 8 that has been attributed to the NADH dehydrogenase fragment mentioned above (Braun *et al.*, 1998). It is assumed that this peak originated from a decay of the entire complex as the fragment does not contain any membranous subunits making it unlikely to be present in the detergent extract from membranes. It is well known that the NADH dehydrogenase fragment tends to dissociate from the residual *E. coli* complex I (Böttcher *et al.*, 2002). No activity peak indicative for the presence of the fully assembled complex was detectable in the gradients loaded with the membrane extract from strains lacking either *nfuA* (Fig. 3A) or *mrp* (Fig. 3B). This is in agreement with the data obtained by native PAGE (Fig. 2) leading to the conclusion that the complex is not stable in these mutants. The additional small activity peak around fraction 10 possibly indicates the presence of another complex I fragment containing NuoF but featuring a higher molecular mass than the NADH dehydrogenase fragment. As this fragment is not detectable in the extract from the parental strain it may stem from a decomposition of the more fragile complex present in the mutants. It does not correspond to the 300 kDa band detected by NBT staining after native PAGE as this band is also detectable in the parental strain (Fig. 2). Surprisingly, the fully assembled complex was not detectable in the sucrose gradient loaded with the extract from the strain lacking *bolA* (Fig. 3C) although a band indicative of the fully assembled complex I was detected after native PAGE (Fig. 2). This might indicate that the complex is fully assembled in the mutant membrane as indicated by its NADH oxidase activity (Table 2) but decays during extraction with 1% detergent due to its diminished stability. Noteworthy, the samples for native PAGE were obtained by extraction with 0.2% dodecyl-maltoside. In addition, the activity profile of the strain lacking *bolA* showed a higher activity peak around fraction 9 (Fig. 3C).

The activity profile obtained with the membrane extract from BW25113 $\Delta ndh \Delta yajL$ showed the activity peak of fully assembled complex I but in a clearly diminished amount (Fig. 3D) consistent with the decreased NADH oxidase activity of the mutant membranes (Table 2) and the NBT staining (Fig. 2). Again, an activity peak around fraction 10 was clearly detectable. The activity profile of the extract from BW25113 $\Delta ndh \Delta grxD$ (Fig. 3E) was similar to that of the *yajL* deletion strain. Here, the small activity peak caused by the entire complex is in agreement with the low amount of complex I detected in this

strain by NBT staining of the native gel (Fig. 3). The strain lacking *ibaG* (Fig. 3F) showed an activity profile similar to that of the parental strain although with slightly reduced activities in accordance with its NADH oxidase activity (Table 2).

The triple deletion of either *ndh/bolA/grxD* (Fig. 3G) or *ndh/bolA/ibaG* (Fig. 3H) led to an activity profile similar to that obtained with the strain devoid of *ndh/bolA* (Fig. 3C). Only the NADH dehydrogenase fragment was detectable in the gradients. In contrast, the fully assembled complex was detectable in the strain lacking *ndh/grxD/ibaG* (Fig. 3I) although the activity of the peak was approximately halved as observed with the strain lacking *ndh/grxD* (Fig. 3E). The strain carrying the quadruple deletion of *ndh/bolA/grxD/ibaG* showed an activity profile similar to that of the strain lacking *ndh* and *bolA*, however, with even less activity in the peaks corresponding to complex I. The activity peak of the NADH dehydrogenase fragment was clearly detectable (Fig. 3J).

Effect of the *mrp* deletion in an *ndh*⁺ background

To validate the results obtained with strain BW25113 Δndh as parental strain, the deletion of *mrp* causing a strong effect on complex I activity and assembly was exemplarily introduced into strain BW25113 and the activity, assembly and stability of the complex in this strain was characterized as described above. BW25113 grew on minimal media with acetate as carbon source similar to BW25113 Δndh . The strain lacking only *mrp* grew like the strain lacking *mrp* and *ndh*, however, worse than the strain lacking *ndh* (Supporting Information, Fig. S4). The NADH oxidase activity of membranes from BW25113 Δmrp was diminished by 10% compared to that of BW25113 (Supporting Information, Table S1), while the d-NADH oxidase activity of BW25113 Δmrp was 25% of its NADH oxidase activity. Thus, halve of the d-NADH oxidase was lost in excellent agreement with the data obtained with BW25113 $\Delta ndh \Delta mrp$ (Table 2). No activity corresponding to the fully assembled complex I was detectable in the gradient loaded with the cleared membrane extract from BW25113 Δmrp (Supporting Information, Fig. S5). An additional activity peak was detected around fraction 6 that is also present in the activity profile of BW25113. This peak is most likely caused by the alternative NADH dehydrogenase that is absent in the other strains. The enzyme/detergent complex is expected to have a molecular mass of about 120 kDa. Again, the results are virtually identical to that obtained with strain BW25113 Δndh demonstrating its excellent suitability to investigate the role of putative cluster carrier proteins for complex I.

Presence of the binuclear Fe/S clusters in the mutant membranes

It was attempted to directly observe the effects caused by the deletion of the putative carrier proteins on the Fe/S clusters of complex I by EPR-spectroscopy. Because of the presence of several membrane-bound proteins containing tetranuclear Fe/S clusters only the signals of the binuclear clusters N1a and N1b can unequivocally be identified when measuring membranes (Dörner *et al.*, 2017). To specifically detect these clusters, difference spectroscopy was applied. Membranes were incubated with 10 μ M piericidin A to prevent reduction of components downstream of the *E. coli* respiratory chain. NADH was added to one aliquot of the membrane suspension while another aliquot was diluted with an equal amount buffer. Spectra of the NADH-reduced and air-oxidized samples were recorded at 40 K and 5 mW microwave power. The spectrum of the oxidized membranes was subtracted from that obtained with the reduced sample. The difference spectrum of the membranes of the parental strain clearly showed the signals of the binuclear clusters N1a and N1b (Fig. 4). The spectral parameters were obtained by simulation (N1a: $g_z = 1.999$, $g_y = 1.95$ and $g_x = 1.925$ and N1b: $g_z = 2.028$, $g_{y,x} = 1.94$). A molar ratio of 1:0.75 was obtained for N1a to N1b as regularly observed under this experimental condition (Leif *et al.*, 1995). The spectra of the mutants lacking YajL, IbaG or GrxD in addition to Ndh did not significantly differ from that obtained with the parental strain (Fig. 4). Accordingly, the mutual deletion of *ibaG* and *grxD* together with *ndh* did not show any effect on the binuclear Fe/S clusters of the complex. However, the difference spectrum of the membranes from the *bolA* deletion strain was very noisy due to a diminished amount of Fe/S clusters in the membrane (Fig. 4). While the signal from N1a was present although with strongly diminished amplitude, no signal from N1b was detectable. Deletion of *nfuA* or *mrp* had no influence on the EPR signals of N1a and N1b suggesting that the low NADH oxidase activity of the membranes from the corresponding strains and the instability of the complex (Figs 2, 3) are due to a loss of tetranuclear Fe/S cluster(s).

Quantification of Nuo-proteins in the *bolA* and *grxD* deletion strains

Unexpectedly, overproduction of GrxD led to a further decrease the NADH oxidase activity (Table 2). To monitor a possible influence of *grxD* on the expression of the *nuo*-genes, the amount of complex I subunits in the *grxD* deletion strain was directly analyzed by quantitative mass spectrometry of cell lysates (Cox and Mann, 2008).

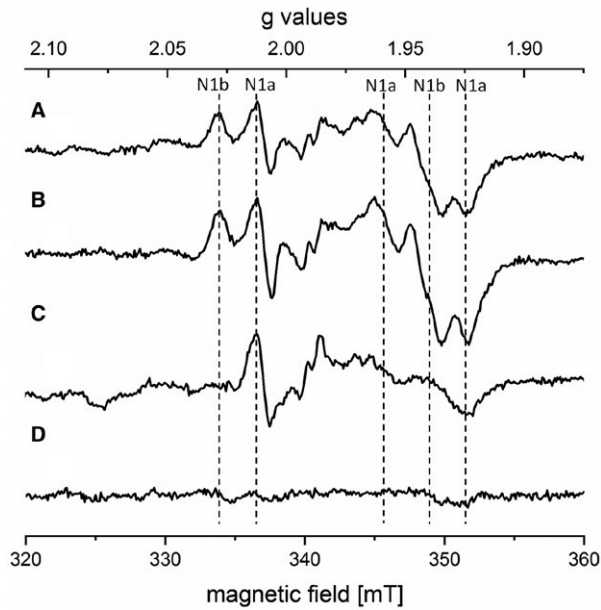


Fig. 4. EPR (NADH-reduced minus air-oxidized) difference spectra of membranes from strain Δndh A. the double deletion strain $\Delta ndh \Delta yajL$ B. the double deletion strain $\Delta ndh \Delta bolA$ C. and from strain Δnuo D. The difference spectra of the other mutant strains were very similar to spectrum (B). The absorptions of the individual clusters are indicated. Other EPR conditions were: microwave frequency, 9.44 GHz; modulation amplitude, 0.6 mT; time constant, 0.164 s; scan rate, 17.9 mT/min.

Furthermore, the amount of complex I subunits was determined in the *bolA* deletion strain, as the complex I activity was only slightly reduced in this strain (Table 2). The content of all Fe/S proteins, namely NuoB, E, F, G and I, of the globular non-Fe/S protein NuoCD and the

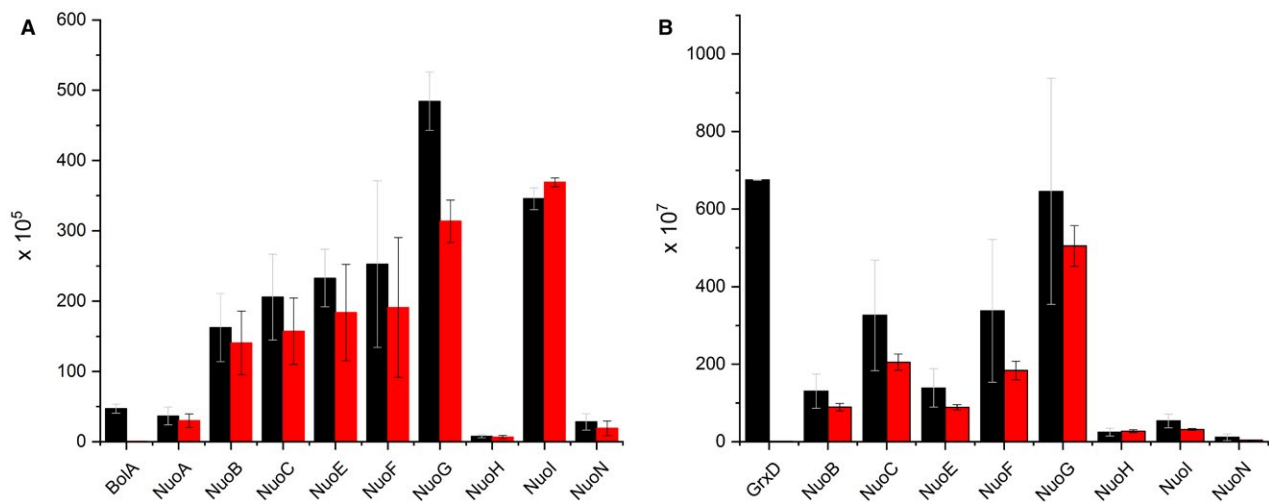


Fig. 5. Mass spectrometric detection of Nuo-subunits in cells from strains lacking *bolA* (A) and *grxD* (B). The intensities of the proteins obtained with the parental strain are shown in black, those from the deletion strains in red.

polytopic non-Fe/S proteins NuoH and N were not significantly altered in the deletion strains compared to that of the parental strain (Fig. 5). Noteworthy, the lack of BolA led to a slight but significant decrease specifically of NuoG that harbours amongst others Fe/S cluster N1b (Fig. 5).

The amount of BolA in the *grxD* deletion strain and the amount of GrxD in the *bolA* deletion strain was not significantly altered compared to their amount in the parental strain. This is noteworthy since it is reported that BolA and GrxD form a complex in *E. coli* (Yeung *et al.*, 2011; Dlouhy *et al.*, 2016).

Discussion

Only little is known about the assembly the *E. coli* complex I especially concerning the incorporation of its Fe/S clusters. It is attempting to speculate that putative Fe/S cluster carrier proteins such as Mrp, NfuA, YajL, BolA and GrxD might be involved in transferring Fe/S cluster(s) from the scaffold protein to the apo-complex. Strain BW25113 Δndh was used as parental strain to generate the knockout strains as it grew indistinguishable from strain BW25113 on minimal acetate medium and enables the direct measurement of complex I activity because NADH is exclusively oxidized by complex I in this strain (Table 1). The deletion of *mrp* in this strain and in BW25113 led to virtually identical results (Supporting Information, Figs S4 and S5, Table S1).

The decreased growth of the strain BW25113 $\Delta ndh \Delta nfuA$ might be caused by a depletion of lipoate in the mutant due to an inactivation of lipoyl synthase (McCarthy and Brooker, 2017). Lipoate is essential for the function

of pyruvate dehydrogenase and 2-oxoglutarate dehydrogenase and, thus, for aerobic growth of *E. coli* (Hermes and Cronan, 2014). However, more important for the poor growth is the significantly decreased level of active complex I as reflected in the diminished NADH oxidase activity (Table 2). The deletion of *ibaG* or *yajL* showed no effect on the growth behaviour in minimal acetate media. The strains complemented with *nfuA*, *mrp* or *grxD* plasmids grew like the parental strain.

Deletion of the eukaryotic Nfu1 causes a diminished amount of Fe/S proteins such as succinate dehydrogenase, aconitase and lipoate synthase (Navarro-Sastre *et al.*, 2011; Ferrer-Cortes *et al.*, 2013; Nizon *et al.*, 2014). Here, we showed that deletion of the *E. coli* homologue *nfuA* also leads to a significantly diminished NADH and succinate oxidase activity that is partially recovered by complementation of the deletion strain with a *nfuA* expression plasmid (Tab. 2). The binuclear Fe/S clusters N1a and N1b were detected in cytoplasmic membranes of the deletion strain by EPR spectroscopy. However, it was not possible to obtain the fully assembled complex I from the membranes even by using mild extraction conditions (Fig. 2). An interaction of NfuA with NuoG was shown by mass spectrometry (Py *et al.*, 2012). NuoG contains three tetranuclear clusters and is, thus, an excellent candidate for interactions with Fe/S cluster carrier proteins. We also detected NfuA together with NuoG in a complex I fragment by mass spectrometry (Fig. S3). Thus, it is very likely that NfuA transfers tetranuclear Fe/S cluster(s) into the complex, although we were not able to determine which and how many of the seven [4Fe-4S] clusters depend on the action of this carrier protein.

Mrp belongs to the Mrp/NBP35 protein family. It was shown that Ind1, another member of this family, is essential for the assembly of mitochondrial complex I (Bych *et al.*, 2008; Sheffel *et al.*, 2009). In *E. coli*, deletion of *mrp* led to a significant decrease complex I activity and stability (Table 2; Figs 2 and 3). In contrast to NfuA, Mrp seems to be specific for complex I assembly since its deletion does not affect succinate oxidase activity. The deletion of Mrp did not affect the incorporation of the binuclear clusters N1a and N1b into the complex suggesting that Mrp like NfuA is involved in the transfer of tetranuclear Fe/S clusters. Due to the low stability of the complex assembled in the mutant, we were not able to identify the clusters that are provided by this Fe/S cluster carrier protein. Taking the data together, Mrp and NfuA are involved in the transfer of tetranuclear Fe/S cluster(s) in complex I with Mrp being specific for complex I.

Membranes from strains lacking *bolA* showed no altered NADH and succinate oxidase activities and complex I assembled in the mutant was extractable with 0.2% detergent (Fig. 2). However, the complex decayed after

extraction with 1% detergent (Fig. 3) and N1b was not detectable in the mutant's membrane by EPR spectroscopy, and the amount of N1a was clearly reduced (Fig. 4). This might indicate that a complex lacking N1b is stable in the membrane but too labile to survive extraction at high detergent concentrations. From calculations of intramolecular electron transfer rates (Page *et al.*, 1999; Moser *et al.*, 2006) it is evident that the loss of N1b will not alter the electron transfer rates from NADH to ubiquinone explaining the consistent NADH oxidase activity of the mutant's membranes. Thus, BolA seems to be specific for the transfer of the binuclear Fe/S cluster N1b into *E. coli* complex I. Since BolA is not capable of binding a Fe/S cluster we propose that it may bind to NuoG guiding the cluster carrier protein to the correct position and possibly assisting the insertion of the cluster into NuoG. There seems to be no specific carrier protein interacting with BolA since the deletion of GrxD had no effect on N1b.

Deletion of the other member of the BolA protein family under investigation here, IbaG, does neither affect the activity nor did the stability of *E. coli* complex I. This is not surprising given the low sequence identity of 22% between BolA and IbaG. Nevertheless, IbaG seemed to play a role for the assembly or the stability of the complex as its amount was slightly but significantly reduced from 3.24 ± 0.16 [U ml⁻¹] to 2.32 ± 0.19 [U ml⁻¹] in the main peak of the sucrose gradient activity profile (Fig. 3).

Using a genetic array analysis Butland and co-workers (2008) observed synthetic sickness and lethality due to deletions of GrxD and BolA-like proteins in strains with mutations within the *isc*-operon suggesting that GrxD and BolA together function in an alternate pathway for Fe/S cluster assembly in *E. coli*. The succinate oxidase activity in membranes from strains lacking either *grxD* and *bolA* or *grxD* and *ibaG* was strongly diminished, while only a mild effect on complex I activity was detectable (Table 2) indicating different importance of the heterodimer for Fe/S cluster incorporation in complex I and II respectively. The GrxD-homodimer as well as the BolA-GrxD-heterodimer are described as [2Fe-2S]-transporters in *E. coli* (Yeung *et al.*, 2011; Li and Outten, 2012). In complex I, deletion of *grxD* did not interfere with the incorporation of the binuclear Fe/S clusters but halved the amount of fully assembled complex I in the detergent extract as indicated by the activity profile of the sucrose gradient (Fig. 3). The NADH oxidase activity was not affected and the succinate oxidase activity was slightly reduced. GrxD is discussed as being part of repair machinery for damaged Fe/S clusters (Boutigny *et al.*, 2013). Thus, it is most likely that GrxD acts as acceptor for damaged Fe/S clusters or as iron or sulfur donor for other chaperones.

Complementation of all strains with plasmids encoding for *bolA*, *ibaG*, *nfuA*, *mrp* and *yajL* leads to an increase in the NADH and succinate oxidase activities (Table 2).

However, the over-expression of *grxD* repeatedly causes a decrease the NADH but not of the succinate oxidase activity in the corresponding strains. The reason for this is still unknown as it is not the result of a possible regulatory function of GrxD (Couturier *et al.*, 2015) as the amount of complex I subunits were unchanged in the mutant cells (Fig. 5).

YajL is reported to interact with complex I subunit NuoG and to play a general role in the protection of *E. coli* proteins against oxidative stress by acting as a covalent chaperone (Le *et al.*, 2012). Cysteine residues that are ligands of Fe/S clusters were proposed to be protected by YajL due to the formation of mixed disulfides. The deletion of *yajL* was reported to lead to a more than sevenfold reduction of the artificial d-NADH/2,6-dichlorophenolindophenol (DCPIP) oxidoreductase activity of *E. coli* membranes, which is interpreted as a 82% loss of complex I (Le *et al.*, 2012; Messaoudi *et al.*, 2015). However, the physiological NADH oxidase activity of the *yajL* deletion strain was decreased just by 22% indicating a much milder effect of the mutation on complex I than proposed (Table 2). Repeating the assay as described by Le *et al.* (2012) the NADH/DCPIP of membranes from strain BW25113 $\Delta ndh \Delta yajL$ were indeed decreased by 80%. However, the absolute activity was very low (0.05 U mg^{-1}) indicating non-optimal assay conditions. By adapting the assay to optimal turnover rates (300 μg membranes, 200 μM NADH) the NADH/DCPIP activity of membranes from the parental strain was determined to $2.46 \pm 0.3 \text{ U mg}^{-1}$, while membranes from strain BW25113 $\Delta ndh \Delta yajL$ showed a just 10 % decreased activity ($2.28 \pm 0.2 \text{ U mg}^{-1}$) in accordance with the NADH oxidase activity described here (Table 2). Nevertheless, only half of complex I activity was detected in the activity profile of the sucrose gradient loaded with an extract from the $\Delta yajL$ strain (Fig. 3). Thus, the lack of YajL led to the formation of complex I that was much more sensitive to the harsh extraction with 1% dodecyl-maltoside from the membrane. Deleting *yajL* did not lead to the loss of a binuclear cluster indicating that YajL might act on the tetranuclear Fe/S clusters. It was proposed that the loss of YajL results in high cellular NADH/NAD⁺ ratio caused by the complex I deficiency that is compensated by upregulation of other dehydrogenases of mixed acid aerobic fermentation (Messaoudi *et al.*, 2015). Indeed, membranes from the $\Delta yajL$ strain show a twofold higher formate oxidase activity indicating a metabolic switch to alternative dehydrogenases (e.g. Fdh-O). Thus, YajL is involved in the assembly of complex I even though it exerts a much milder effect as proposed (Le *et al.*, 2012).

To answer the question whether one of the putative Fe/S cluster carrier proteins might also regulate protein biosynthesis e.g. by acting as transcription factor as reported for BolA (Dressaire *et al.*, 2015) the amount of

the Nuo-proteins in the strain lacking *bolA* were determined *via* mass spectrometry (Fig. 5). The lack of BolA led to a slight decrease the level of NuoG to $65\% \pm 10\%$ to that of the parental strain. This is in line with lack of Fe/S cluster N1b being located on NuoG in this strain.

Experimental procedures

Strains, plasmids and oligonucleotides

All *E. coli* strains, plasmids, and oligonucleotides used in this work are listed in Tables S2–S4 respectively. Deletion strains were constructed as described (Datsenko and Wanner, 2000). The linear fragments were generated by PCR using primers with 36–50 nt extensions that are homologous to regions adjacent to the gene to be inactivated. The resistance gene (*nptII*) with FLP recognition target sites was introduced with the phage λ Red recombinase, which is carried by the pKD46 plasmid under the control of an inducible arabinose promoter. The resistance genes were then eliminated by using the *pcp20* plasmid encoding the flippase (FLP) recombinase. Genomic mutations and newly generated vectors were checked by sequencing (GATC biotech). Restriction and DNA-modifying enzymes were obtained from Fermentas.

Cell growth and isolation of cytoplasmic membranes

E. coli cells were grown aerobically at 37°C in baffled flasks using minimal media (Miller, 1992) with 25 mM acetate or 25 mM glucose as sole carbon source while agitating at 180 r.p.m. Every growth was performed three times and an error of ± 5 –8% was determined. The error bars are not shown in the figures due to clarity. Cells for the isolation of cytoplasmic membranes were grown on phosphate-buffered LB-medium. Strains containing a plasmid were grown in the presence of ampicillin ($100 \mu\text{g ml}^{-1}$). Cells were harvested by centrifugation ($5,700 \times g$, 10 min, 4°C, Rotor JLA 8.1000, Avanti J-26 XP, Beckman Coulter) in the exponential phase yielding approximately $6.5 \text{ g cells l}^{-1}$. All further steps were carried out at 4°C. Five grams of the cell sediment were suspended in fourfold volume of 50 mM MES/NaOH, pH 6.0, 50 mM NaCl, 0.1 mM PMSF supplemented with a few grains of desoxyribonuclease I and disrupted by passing twice through a French Pressure Cell Press (110 MPa, SLM-Aminco). Cell debris and non-disrupted cells were removed by centrifugation ($9,500 \times g$, 20 min, 4°C, Rotor A8.24, RC-5 Superspeed Refrigerated Centrifuge, Sorvall Instruments). Cytoplasmic membranes were obtained from the supernatant by centrifugation at $160,000 \times g$ (60 min, 4°C, Rotor 60Ti, L8-M Ultrafuge, Beckman). The sediment was suspended in an equal volume (1:1, w/v) of the buffer mentioned above and either immediately used or frozen in liquid nitrogen and stored at -80°C .

Activity assays

The NADH and succinate oxidase activity of cytoplasmic membranes were measured with a Clarke-type oxygen electrode (DW1, Hansatech) at 30°C in a volume of 2 ml.

To calibrate the electrode 2 ml water were deoxygenized by adding sodium dithionite and the signal was set to 237 mM oxygen (Weiss *et al.*, 1970). The assay contained 5 μ l cytoplasmic membranes and the reaction was started by the addition of the corresponding substrate (1.25 mM NADH, 10 mM succinate) after obtaining a constant baseline. The substrate/ferricyanide oxidoreductase activities were measured as the decrease in the absorbance of ferricyanide at 410 nm with an Ultraspec spectrophotometer (Amersham Pharmacia Biotech, Munich, Germany) in a volume of 1 ml. The assay contained 5 μ l membrane suspension or 50 μ l of a fraction after sucrose gradient centrifugation. The reaction was started by an addition of either 0.2 mM NADH or 1 mM succinate. Every measurement was done in duplicates from 2 to 3 independent cell growths. An error of \pm 5–8% was determined. The NADH/DCPIP assay was performed as described (Messaudi *et al.*, 2015).

Sucrose gradient centrifugation

Membrane proteins were solubilized by an addition of 1% (w/v) n-dodecyl- β -D-maltopyranoside (DDM; Neofroxx) at 4°C. The extract was centrifuged for 20 min at 160,000 \times g and 4°C (Rotor 60Ti, L8-M Ultrafuge, Beckman). 2 ml of the supernatant were loaded onto 24 ml gradients of 5–30% (w/v) sucrose and centrifuged for 16 h at 140,000 \times g (4°C, Rotor SW28, L8-M Ultrafuge, Beckman). The gradients were fractionated into 1 ml portions and the substrate/ferricyanide oxidoreductase activities were determined as described above. Every measurement was done as duplicate with membranes isolated from two independent cell growths. An error of \pm 6–10% was determined. The error bars are not shown in the figures due to clarity.

Native acrylamide gel electrophoresis

A 3.5–16% polyacrylamide gel was poured. MES (30 mM) and histidine (30 mM) were used as buffers. Membrane proteins were solubilized by an addition of 0.2% (w/v) DDM (Neofroxx) at 4°C over night. After centrifugation for 20 min at 160,000 \times g and 4°C (Rotor 60Ti, L8-M Ultrafuge, Beckman) the samples were mixed with glycerol and Ponceau S. The gel was run at 4°C and 15 mA. For staining the gel was incubated for 5 min with 1 mg ml⁻¹ NBT in 100 mM MOPS, pH 8 and the reaction was started by an addition of 100 μ M NADH.

Mass spectrometry

Bacteria were grown aerobically on minimal medium (33.7 mM NaHPO₄ (w/v), 22 mM KH₂PO₄ (w/v), 8.55 mM NaCl (w/v), 9.35 mM NH₄Cl (w/v), 0.4% glucose (w/v), 1 mM MgSO₄ (w/v), 0.3 mM CaCl₂ (w/v), 1 μ g thiamin, 0.13 mM EDTA (w/v), 25 μ M FeCl₃ (w/v), 6.2 μ M ZnCl₂ (w/v), 0.76 μ M CuCl₂ (w/v), 0.42 μ M CoCl₂ (w/v), 1.62 μ M H₃BO₄ (w/v), 0.08 μ M MnCl₂ (w/v)) until the Mid-log phase. After washing in 50 mM Tris-HCl, pH 8.0, bacterial cells were suspended in 50 mM Tris-HCl, 150 mM NaCl and 0.5 NP-40, pH 8.0 and sonicated. 100 μ g protein lysate was mixed with 8 M urea in 10 mM Tris-HCl, pH 8.0 and loaded on filter column (Microcon-30 kDa Centrifugal Filter Unit with Ultracel-30

membrane). Columns were washed with 8 M Urea in 10 mM Tris-HCl, pH 8.0, 10 mM DTT in 8 M Urea in 10 mM Tris-HCl, pH 8.0 and 27 mM iodoacetamide in 10 mM Tris-HCl, pH 8.0. Columns were mixed at 600 r.p.m. in a thermomixer for 1 min and incubated without mixing for further 5 min. Eight molars of urea in 10 mM Tris-HCl pH 8.0 was added to each column and the column was centrifuged. After this step, samples were digested for 14 h with trypsin. Peptides were purified on C18 SepPack columns (Teknokroma) and eluted with 800 μ l 60% ACN, 0.1% TFA, dried in the speed vacuum concentrator and stored at -80°C prior to mass spectrometry analysis. Measurements were performed on a Q Exactive HF mass spectrometer coupled with a nLC1000 nano-HPLC (both Thermo Scientific). Quantitative analysis of MS/MS measurements was performed with Progenesis LC/MS software (Nonlinear Dynamics) and MaxQuant software (Cox and Mann, 2008). The following settings for both programs were used for a search: 10 ppm peptide mass tolerance; 0.8 Da MS/MS tolerance; maximum of two missed cleavages allowed, threshold for validation of peptides set to 0.01 using a decoy database, carbamidomethylation of cysteine was set as a fixed modification and oxidation of methionine was set as variable modification. While analyzing data with MaxQuant the “label-free quantification” and “match between runs” options were selected. The minimum peptide length of six amino acids was used. The quantification was performed for proteins with minimum of one unique and one razor peptide. Known contaminants such as keratins were removed from further analysis. While data analysis with Progenesis software peptide identifications with a Mascot score below 25 were excluded. Mascot results were imported into Progenesis Q1, quantitative peak area information extracted and the results exported for further analysis.

EPR spectroscopy

Twenty milligrams of cytoplasmic membranes were mixed with 1 μ l piericidin A (10 mM). One aliquot was reduced by an addition of 5 mM NADH. Another aliquot was diluted by an addition of the same volume buffer. Spectra of the NADH-reduced and air-oxidized samples were recorded at 40 K and 5 mW microwave power. The spectrum of the oxidized membranes was subtracted from that obtained with the reduced sample.

Acknowledgements

This work was funded by the Deutsche Forschungsgemeinschaft (DFG) through GRK 1976, GRK 2202, SPP 1927 (FR 1140/11-1) and the Spemann Graduate School of Biology and Medicine (SGBM). We thank the ZBSA (Zentrum für Biosystemanalyse, University Freiburg) for the mass spectrometric analysis of the novel complex I fragment. The authors declare no conflicts of interests.

Author contributions

SB, DKD and FN made the mutants and measured oxidase activities; SB, MH and MS grew the cells; SB, FN, MH and

MS performed sucrose gradient centrifugation; SB performed native PAGE, TF performed the EPR spectroscopy; AZ, BS and MG performed the MS analysis; SB, DKD, FN, SL and TF analyzed the data; SB and TF wrote the paper; TF designed the project.

References

- Agar, J., Yuvaniyama, P., Jack, R., Cash, V., Smith, A., Dean, D. *et al.* (2000) Modular organization and identification of a mononuclear iron-binding site within the NifU protein. *JBIC Journal of Biological Inorganic Chemistry*, **5**, 167–177.
- Ayala-Castro, C., Saini, A. and Outten, F. (2008) Fe-S cluster assembly pathways in bacteria. *Microbiology and Molecular Biology Reviews*, **72**, 110–125.
- Angelini, S., Gerez, C., Ollagnier-de Choudens, S., Sanakis, Y. *et al.* (2008) NfuA, a new factor required for maturing Fe/S proteins in *Escherichia coli* under oxidative stress and iron starvation conditions. *The Journal of Biological Chemistry*, **283**, 14084–14091.
- Baertling, F., Sánchez-Caballero, L., van den Brand, M., Wintjes, L., Brink, M. *et al.* (2017) NDUFAF4 variants are associated with Leigh syndrome and cause a specific mitochondrial complex I assembly defect. *European Journal of Human Genetics*, **25**, 1273–1277.
- Bandyopadhyay, S., Chandramouli, K. and Johnson, M. (2008) Iron-sulfur cluster biosynthesis. *Biochemical Society Transactions*, **36**, 1112–1119.
- Baradaran, R., Berrisford, J., Minhas, G. and Sazanov, L. (2013) Crystal structure of the entire respiratory complex I. *Nature*, **494**, 441–445.
- Baranova, E., Morgan, D. and Sazanov, L. (2007) Single particle analysis confirms distal location of subunits NuoL and NuoM in *Escherichia coli* complex I. *Journal of Structural Biology*, **159**, 238–242.
- Bidichandani S., and Delatycki, M. (1998) Friedreich Ataxia. In: Adam, M.P., Ardinger, H.H., Pagon, R.A., Wallace, S.E., Bean, L.J.H., Stephens, K., Amemiya, A. (Eds.) *GeneReviews*. Seattle, WA: University of Washington, pp. 1993–2018.
- Birrell, J., Morina, K., Bridges, H., Friedrich, T. and Hirst, J. (2013) Investigating the function of [2Fe-2S] cluster N1a, the off-pathway cluster in complex I, by manipulating its reduction potential. *Biochemical Journal*, **456**, 139–146.
- Boutigny, S., Saini, A., Baidoo, E.E., Yeung, N., Keasling, J.D. and Butland, G. (2013) Physical and functional interactions of a monothiol glutaredoxin and an iron sulfur cluster carrier protein with the sulfur-donating radical S-adenosyl-L-methionine enzyme MiaB. *The Journal of Biological Chemistry*, **288**, 14200–14211.
- Boyd, J., Drevland, R., Downs, D. and Graham, D. (2008) Archaeal ApbC/Nbp35 homologs function as iron-sulfur cluster carrier proteins. *Journal of Bacteriology*, **191**, 1490–1497.
- Böttcher, B., Scheide, D., Hesterberg, M., Nagel-Steger, L. and Friedrich, T. (2002) A novel, enzymatically active conformation of the *Escherichia coli* NADH:ubiquinone oxidoreductase (complex I). *The Journal of Biological Chemistry*, **277**, 17970–17977.
- Braun, M., Bungert, S. and Friedrich, T. (1998) Characterization of the overproduced NADH dehydrogenase fragment of the NADH:ubiquinone oxidoreductase (complex I) from *Escherichia coli*. *Biochemistry*, **37**, 1861–1867.
- Braymer, J. and Lill, R. (2017) Iron-sulfur cluster biogenesis and trafficking in mitochondria. *Journal of Biological Chemistry*, **292**, 12754–12763.
- Butland, G., Babu, M., Diaz-Mejia, J.J., Bohdana, F., Phanse, S., Gold, B. *et al.* (2008) *E. coli* synthetic genetic array analysis. *Nature Methods*, **5**, 789–795.
- Bych, K., Kerscher, S., Netz, D., Pierik, A., Zwicker, K. *et al.* (2008) The iron-sulphur protein Ind1 is required for effective complex I assembly. *The EMBO Journal*, **27**, 1736–1746.
- Couturier, J., Przybyla-Toscano, J., Roret, T., Didierjean, C. and Rouhier, N. (2015) The roles of glutaredoxins ligating Fe-S clusters: Sensing, transfer or repair functions? *Biochimica et Biophysica Acta (BBA)*, **1853**, 1513–1527.
- Cox, J. and Mann, M. (2008) MaxQuant enables high peptide identification rates, individualized p.p.b.-range mass accuracies and proteome-wide protein quantification. *Nature Biotechnology*, **26**, 1367–1372.
- Datsenko, K. and Wanner, B. (2000) One-step inactivation of chromosomal genes in *Escherichia coli* K-12 using PCR products. *Proceedings of the National Academy of Sciences of the United States of America*, **97**, 6640–6645.
- de Vries, S., Dörner, K., Strampraad, M. and Friedrich, T. (2015) Electron tunneling rates in respiratory complex I are tuned for efficient energy conversion. *Angewandte Chemie International Edition*, **54**, 2844–2848.
- Dlouhy, A., Li, H., Albetel, A., Zhang, B., Mapolelo, D. *et al.* (2016) The *Escherichia coli* BolA Protein IbaG Forms a Histidine-Ligated [2Fe-2S]-Bridged Complex with Grx4. *Biochemistry*, **55**, 6869–6879.
- Dos Santos, P., Smith, A., Frazzon, J., Cash, V., Johnson, M. and Dean, D. (2004) Iron-sulfur cluster assembly: NifU-directed activation of the nitrogenase Fe protein. *Journal of Biological Chemistry*, **279**, 19705–19711.
- Dörner, K., Vranas, M., Schimpf, J., Straub, I., Hoerer, J. and Friedrich, T. (2017) Significance of [2Fe-2S] Cluster N1a for Electron Transfer and Assembly of *Escherichia coli* Respiratory Complex I. *Biochemistry*, **56**, 2770–2778.
- Dressaire, C., Moreira, R., Barahona, S., Alves de Matos, A. and Arraiano, C. (2015) BolA is a transcriptional switch that turns off motility and turns on biofilm development. *mBio*, **6**, e02352–14.
- Ferrer-Cortes, X., Font, A., Bujan, N., Navarro-Sastre, A., Matalonga, L. *et al.* (2013) Protein expression profiles in patients carrying NFU1 mutations. Contribution to the pathophysiology of the disease. *Journal of Inherited Metabolic Disease*, **36**, 841–847.
- Fiedorczuk, K., Letts, J.A., Degliesposti, G., Kaszuba, K., Skehel, M. and Sazanov, L.A. (2016) Atomic structure of the entire mammalian mitochondrial complex I. *Nature*, **538**, 406–410.
- Friedrich, T., van Heek, P., Leif, H., Ohnishi, T., Forche, E., Kunze, B. *et al.* (1994) Two binding sites of inhibitors in

- NADH:ubiquinone oxidoreductase (complex I). *European Journal of Biochemistry*, **219**, 691–698.
- Friedrich, T. (2014) On the mechanism of respiratory complex I. *Journal of Bioenergetics and Biomembranes*, **46**, 255–268.
- Friedrich, T., Kreuzer Dekovic, D. and Burschel, S. (2016) Assembly of the *Escherichia coli* NADH:ubiquinone oxidoreductase. *Biochimica et Biophysica Acta*, **1857**, 214–223.
- Gautier, V., Le, H., Malki, A. and Messaoudi, N. (2012) YajL, the prokaryotic homolog of the Parkinsonism-associated protein DJ-1, protects cells against protein sulfenylation. *Journal of Molecular Biology*, **421**, 662–670.
- Gnandt, E., Schimpf, J., Harter, C., Hoesser, J. and Friedrich, T. (2017) Reduction of the off-pathway iron-sulphur cluster N1a of *Escherichia coli* respiratory complex I restrains NAD⁺ dissociation. *Scientific Reports*, **7**, 8754.
- Hattab, G., Warschawski, D., Moncoq, K. and Miroux, B. (2015) *Escherichia coli* as host for membrane protein structure determination: a global analysis. *Scientific Reports*, **5**, 12097.
- Hausmann, A., Netz, D. and Balk, J. (2005) The eukaryotic P loop NTPase Nbp35: an essential component of the cytosolic and nuclear iron-sulfur protein assembly machinery. *Proceedings of the National Academy of Sciences of the United States of America*, **102**, 3266–3271.
- Hermes, F. and Cronan, J. (2014) An NAD synthetic reaction bypasses the lipoate requirement for aerobic growth of *Escherichia coli* strains blocked in succinate catabolism. *Molecular Microbiology*, **94**, 1134–1145.
- Isaya, G. (2014) Mitochondrial iron-sulfur cluster dysfunction in neurodegenerative disease. *Frontiers in Pharmacology*, **5**, 1–7.
- Jin, Z., Heinnickel, M., Krebs, C., Shen, G., Golbeck, J. and Bryant, D. (2008) Biogenesis of iron-sulfur clusters in photosystem I: holo-NfuA from the cyanobacterium *Synechococcus* sp. PCC 7002 rapidly and efficiently transfers [4Fe-4S] clusters to apo-PsaC *in vitro*. *Journal of Biological Chemistry*, **283**, 28426–28435.
- John, P. (1976) Aerobic and anaerobic bacterial respiration monitored by electrodes. *Journal of General Microbiology*, **98**, 231–238.
- Koonin, E. (1993) A superfamily of ATPases with diverse functions containing either classical or deviant ATP-binding motif. *Journal of Molecular Biology*, **229**, 1165–1174.
- Kiley, P. and Beinert, H. (2003) The role of Fe-S proteins in sensing and regulation in bacteria. *Current Opinion in Microbiology*, **6**, 181–185.
- Le, H., Gautier, V., Kthiri, F., Malki, A. and Messaoudi, N. (2012) YajL, prokaryotic homolog of parkinsonism-associated protein DJ-1, functions as a covalent chaperone for thiol proteome. *Journal of Bacteriology*, **287**, 5861–5870.
- Leif, H., Sled, V.D., Ohnishi, T., Weiss, H. and Friedrich, T. (1995) Isolation and characterization of the proton-translocating NADH: ubiquinone oxidoreductase from *Escherichia coli*. *European Journal of Biochemistry*, **230**, 538–548.
- Li, H. and Outten, C. (2012) Monothiol CGFS glutaredoxins and BolA-like proteins: [2Fe-2S] binding partners in iron homeostasis. *Biochemistry*, **51**, 4377–4389.
- Lin, M.T. and Beal, M.F. (2006) Mitochondrial dysfunction and oxidative stress in neurodegenerative diseases. *Nature*, **443**, 787–795.
- Loiseau, L., Gerez, C., Bekker, M., Ollagnier-de Choudens, S., Py, B. et al. (2007) ErpA, an iron sulfur (FeS) protein of the A-type essential for respiratory metabolism in *Escherichia coli*. *Proceedings of the National Academy of Sciences of the United States of America*, **104**, 13626–13631.
- McCarthy, E.L. and Booker, S.J. (2017) Destruction and reformation of an iron-sulfur cluster during catalysis by lipoyl synthase. *Science*, **358**, 373–377.
- Melber, A., Na, U., Vashisht, A., Weiler, B., Lill, R. et al. (2016) Role of Nfu1 and Bol3 in iron-sulfur cluster transfer to mitochondrial clients. *eLife*, **5**, e15991.
- Messaoudi, N., Gautier, V., Dairou, J., Mihoub, M., Lelandais, G. et al. (2015) Fermentation and alternative respiration compensate for NADH dehydrogenase deficiency in a prokaryotic model of DJ-1-associated Parkinsonism. *Microbiology*, **161**, 2220–2231.
- Miller, J. (1992) *A Short Course in Bacterial Genetics*. Cold Spring Harbor: Cold Spring Harbor Laboratory.
- Mihara, H. and Esaki, N. (2002) Bacterial cysteine desulfurases: their function and mechanisms. *Applied Microbiology and Biotechnology*, **60**, 12–23.
- Moser, C., Farid, T., Chobot, S. and Dutton, L. (2006) Electron tunneling chains of mitochondria. *Biochimica et Biophysica Acta (BBA)*, **1757**, 1096–1109.
- Nachin, L., Loiseau, L., Expert, D. and Barras, F. (2003) SufC: an unorthodox cytoplasmic ABC/ATPase required for [Fe-S] biogenesis under oxidative stress. *The EMBO Journal*, **22**, 427–437.
- Navarro-Sastre, A., Tort, F., Stehling, O., Uzarska, M.A., Arranz, J.A. et al. (2011) A fatal mitochondrial disease is associated with defective NFU1 function in the maturation of a subset of mitochondrial Fe-S proteins. *The American Journal of Human Genetics*, **89**, 656–667.
- Nizon, M., Boutron, A., Boddaert, N., Slama, A., Delpech, H. et al. (2014) Leukoencephalopathy with cysts and hyperglycinemia may result from NFU1 deficiency. *Mitochondrion*, **15**, 59–64.
- Ohnishi, T. and Nakamaru-Ogiso, E. (2008) Where there any “misassignments” among iron-sulfur clusters N4, N5 and N6b in NADH-quinone oxidoreductase (complex I)? *Biochimica et Biophysica Acta*, **1777**, 703–710.
- Page, C., Moser, C., Chen, X. and Dutton, P. (1999) Natural engineering principles of electron tunnelling in biological oxidation-reduction. *Nature*, **402**, 47–52.
- Pohl, T., Walter, J., Stolpe, S., Soufo, J., Grauman, P. and Friedrich, T. (2007a) Effects of the deletion of the *Escherichia coli* frataxin homologue CyaY on the respiratory NADH:ubiquinone oxidoreductase. *BMC Biochemistry*, **24**, 8–13.
- Pohl, T., Bauer, T., Dörner, K., Stolpe, S., Sell, P., Zocher, G. and Friedrich, T. (2007b) Iron-sulfur cluster N7 of the NADH:ubiquinone oxidoreductase (complex I) is essential for stability but not involved in electron transfer. *Biochemistry*, **46**, 6588–6596.

- Py, B. and Barras, F. (2010) Building Fe-S proteins: bacterial strategies. *Nature Reviews Microbiology*, **8**, 436–446.
- Py, B., Gerez, C., Angelini, S., Planel, R., Vinella, D. *et al.* (2012) Molecular organization, biochemical function, cellular role and evolution of NfuA, an atypical Fe-S carrier. *Molecular Microbiology*, **86**, 155–171.
- Py, B. and Barras, F. (2015) Genetic approaches of the Fe-S cluster biogenesis process in bacteria: Historical account, methodological aspects and future challenges. *Biochimica et Biophysica Acta*, **1853**, 1429–1435.
- Rhein, V., Song, X., Wiesner, A., Ittner, L.M., Baysang, G. *et al.* (2009) Amyloid- β and tau synergistically impair the oxidative phosphorylation system in triple transgenic Alzheimer's disease mice. *Proceedings of the National Academy of Sciences of the United States of America*, **106**, 20057–20062.
- Roche, B., Aussel, L., Ezraty, B., Mandin, P., Py, B. and Barras, F. (2013) Iron/sulfur proteins biogenesis in prokaryotes: Formation, regulation and diversity. *Biochimica et Biophysica Acta (BBA)*, **1827**, 455–469.
- Sastry, M., Korotkov, K., Brodsky, Y. and Baneyx, F. (2002) Hsp31, the *Escherichia coli* yedU gene product, is a molecular chaperone whose activity is inhibited by ATP at high temperatures. *Journal of Biological Chemistry*, **277**, 46026–46034.
- Schwartz, C., Djaman, O., Imlay, J. and Kiley, P. (2000) The cysteine desulfurase, IscS, has a major role in *in vivo* Fe-S cluster formation in *Escherichia coli*. *Proceedings of the National Academy of Sciences of the United States of America*, **97**, 9009–9014.
- Sheftel, A., Stehling, O., Pierik, A., Netz, D. and Kerscher, S. (2009) Human Imd1, an iron- sulfur cluster assembly factor for respiratory complex I. *Molecular and Cellular Biology*, **29**, 6059–6073.
- Smith, A., Jameson, G., Dos Santos, P. and Agar, J. (2005) NifS-mediated assembly of [4Fe- 4S] clusters in the N- and C-terminal domains of the NifU scaffold protein. *Biochemistry*, **44**, 12955–12969.
- Takahashi, Y. and Tokumoto, U. (2002) A third bacterial system for the assembly of iron- sulfur clusters with homologs in archaea and plastids. *Journal of Biological Chemistry*, **277**, 28380–28383.
- Tan, G., Lu, J., Bitoun, J.P., Huang, H. and Ding, H. (2009) IscA/SufA paralogues are required for the [4Fe-4S] cluster assembly in enzymes of multiple physiological pathways in *Escherichia coli* under aerobic growth conditions. *Biochemical Journal*, **420**, 463–472.
- Uden, G., Steinmetz, P. and Degreif-Dünnwald, P. (2014) The aerobic and anaerobic respiratory chain of *Escherichia coli* and *Salmonella enterica*: enzymes and energetics. *EcoSal Plus*. <https://doi.org/10.1128/ecosalplus.ESP-0005-2013>
- Uzarska, M., Nasta, V., Weiler, B., Spantgar, F., Ciofi-Baffoni, S. *et al.* (2016) Mitochondrial Bol1 and Bol3 function as assembly factors for specific iron-sulfur proteins. *eLife*, **5**, e16673.
- Vinella, D., Brochier-Armanet, C., Loiseau, L., Talla, E. and Barras, F. (2009) Iron-sulfur (Fe/S) protein biogenesis: phylogenomic and genetic studies of A-type carriers. *PLoS Genetics*, **5**, e1000497.
- Weiss, H., von Jagow, G., Klingenberg, M. and Bücher, T. (1970) Characterization of *Neurospora crassa* mitochondria prepared with a grind-mill. *European Journal of Biochemistry*, **14**, 75–82.
- Yakovlev, G., Reda, T. and Hirst, J. (2007) Reevaluating the relationship between EPR spectra and enzyme structure for the iron-sulfur clusters in NADH:quinone oxidoreductase. *Proceedings of the National Academy of Sciences of the United States of America*, **104**, 12720–12725.
- Yankovskaya, V., Horsefield, R., Törnroth, S., Luna-Chavez, C., Miyoshi, H. *et al.* (2003) Architecture of succinate dehydrogenase and reactive oxygen species generation. *Science*, **299**, 700–704.
- Yeung, N., Gold, B., Liu, N., Prathapam, R., Sterling, H., Williams, E. *et al.* (2011) The *E. coli* monothiol glutaredoxin GrxD forms homodimeric and heterodimeric FeS cluster containing complexes. *Biochemistry*, **41**, 8957–8969.
- Zheng, L. and Dean, D. (1994) Catalytic formation of a nitrogenase iron-sulfur cluster. *Journal of Biological Chemistry*, **269**, 18723–18726.
- Zhu, J., Vinothkumar, K.R. and Hirst, J. (2016) Structure of mammalian respiratory complex I. *Nature*, **536**, 354–358.
- Zerbetto, E., Vergani, L. and Dabbeni-Sala, F. (1997) Quantification of muscle mitochondrial oxidative phosphorylation enzymes via histochemical staining of blue native polyacrylamide gels. *Electrophoresis*, **18**, 2059–2064.
- Zickermann, V., Wirth, C., Nasiri, H., Siegmund, K., Schwalbe, H., Hunte, C. and Brandt, U. (2015) Mechanistic insight from the crystal structure of mitochondrial complex I. *Science*, **347**, 44–49.

Supporting information

Additional supporting information may be found online in the Supporting Information section at the end of the article.